EBSD Explained

From data acquisition to advanced analysis

OXFORD INSTRUMENTS

The Business of Science®

Introduction

Electron Backscatter Diffraction (EBSD) is a scanning electron microscope (SEM) based technique that gives crystallographic information about the microstructure of a sample. In EBSD, a stationary electron beam interacts with a tilted crystalline sample and the diffracted electrons form a pattern that can be detected with a fluorescent screen. The diffraction pattern is characteristic of the crystal structure and orientation in the sample region where it was generated. Hence the diffraction pattern can be used to determine the crystal orientation, discriminate between crystallographically different phases, characterise grain boundaries, and provide information about the local crystalline perfection.

When the electron beam is scanned in a grid across a polycrystalline sample and the crystal orientation is measured at each point, the resulting map reveals the grain morphology, orientations and boundaries. This data can also be used to show the preferred crystal orientation (i.e. texture) within the sample. Thus a complete and quantitative representation of the microstructure can be established with EBSD.

EBSD has become a well established accessory for the SEM, which is used to provide crystallographic information routinely. As a result, EBSD is now being applied in numerous different application areas to assist in materials characterisation, as shown by the table below.

Sample preparation is critical to obtaining good EBSD results; a deformation-free surface is required to yield good electron backscattered diffraction patterns (EBSPs). More information on this subject is available on www.ebsd.com.

This guide describes how an EBSD system works, and gives examples of the type of results EBSD can generate.

Cover: Equal Channel Angular Pressed (ECAP) deformed Al alloy showing the Inverse Pole Figure Z direction on top of the pattern quality, with high angle boundaries in black and low angle (3-10º) in grey. Step size 7.5 nm. Courtesy: Morgan Tort (University of Melbourne) and Pat Trimby (University of Sydney).

Industries	Materials	Typical EBSD Measurements
Metals research and processing	Metals, Alloys	Grain size
Aerospace	Intermetallics	Grain boundary characterisation
Automotive	Inclusions / precipitates / 2nd phases	Global texture
Nuclear	Ceramics	Local texture
Microelectronics	Thin Films	CSL boundary charcterisation
Earth Science	Solar Cells	Recrystallised / deformed fractions
Academia	Geological	Substructure analysis
	Semiconductors	Phase identification
	Superconductors	Phase fractions / distributions
	Ice	Phase transformation
	Metal / ceramic composites	Fracture analysis
	Bone, teeth	Orientation & misorientation relationships between grains / phases

Table 1. A summary of the different application areas and the typical types of measurement made using EBSD.

Basics of EBSD

Principle system components

A typical EBSD setup (Fig. 1) consists of:

- A crystalline sample tilted to 70º from horizontal, by use of the SEM stage or a pretilted holder.
- A phosphor screen, which is fluoresced by the electrons scattered from the sample.
- A sensitive camera together with optics for viewing the pattern formed on the phosphor screen.
- An insertion mechanism, which accurately controls the position of the detector when it is in use, and retracts the detector to a safe position when it's not in use to prevent interference with SEM operation.
- Electronics to control the SEM, including the beam and stage movements.
- A computer to control the EBSD experiments, collect and analyse the diffraction patterns, and display the results.
- Optional forescatter diodes (FSD) mounted around the phosphor screen, which are used to generate microstructure images of the sample before collecting EBSD data.

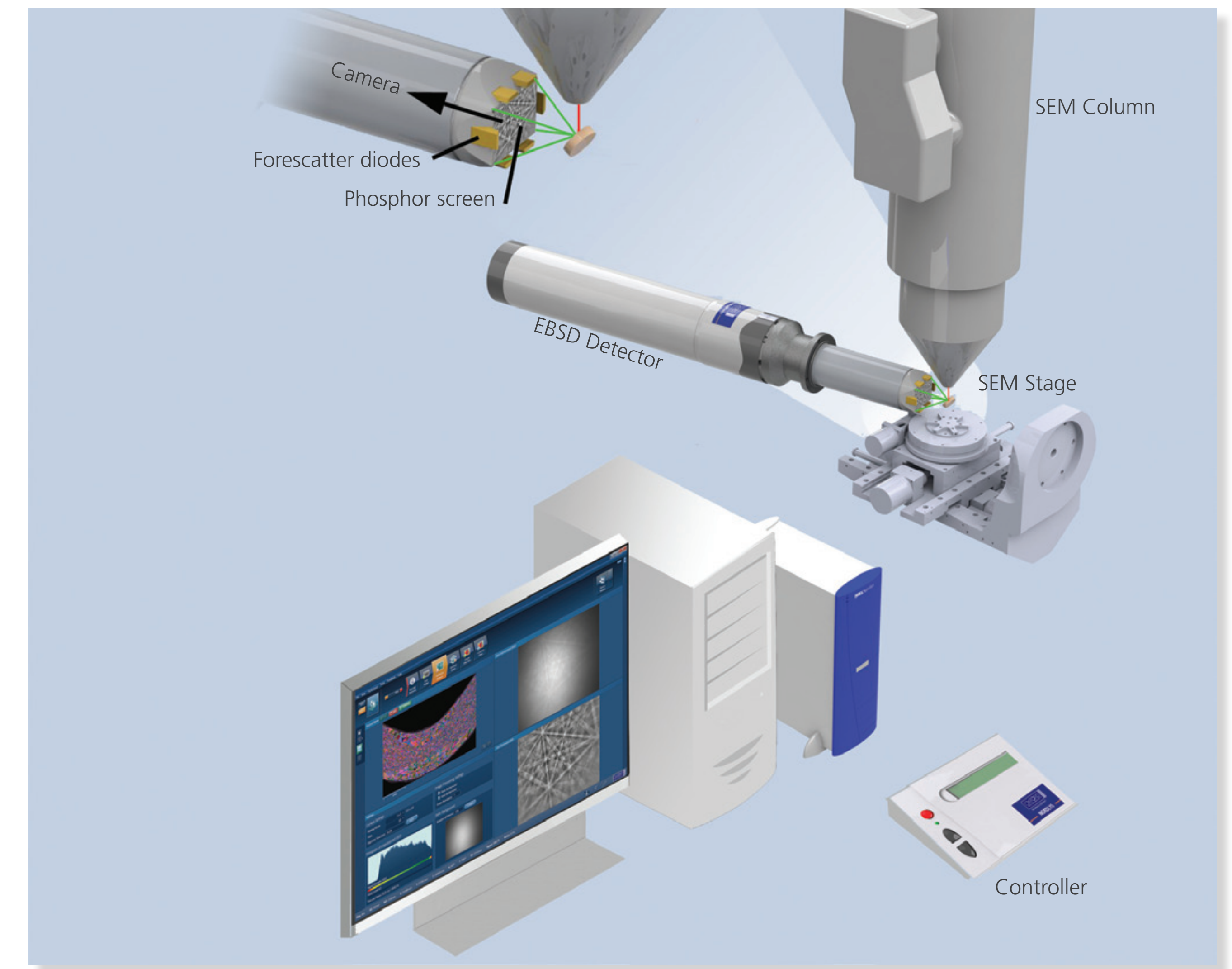

Fig. 1. The principle components of an EBSD system.

Basics of EBSD...

Pattern formation and detection

The following model describes the principle features of pattern formation and detection for EBSD analysis. A beam of electrons is directed at a point of interest on a tilted crystalline sample. The atoms in the material inelastically scatter a fraction of the electrons, with a small loss of energy, to form a divergent source of electrons close to the surface of the sample. Some of these electrons are incident on atomic planes at angles that satisfy the Bragg equation:

$$n\lambda = 2dSin\theta$$

where n is an integer, λ is the wavelength of the electrons, d is the spacing of the diffracting plane, and θ the angle of incidence of the electrons on the diffracting plane.

These electrons are diffracted to form a set of paired large-angle cones that correspond to each diffracting plane. The image produced on the phosphor screen contains characteristic Kikuchi bands which are formed where the regions of enhanced electron intensity intersect the screen (Fig. 2). The pattern seen is a gnomonic projection of the diffracted cone, making the band edges appear hyperbolic.

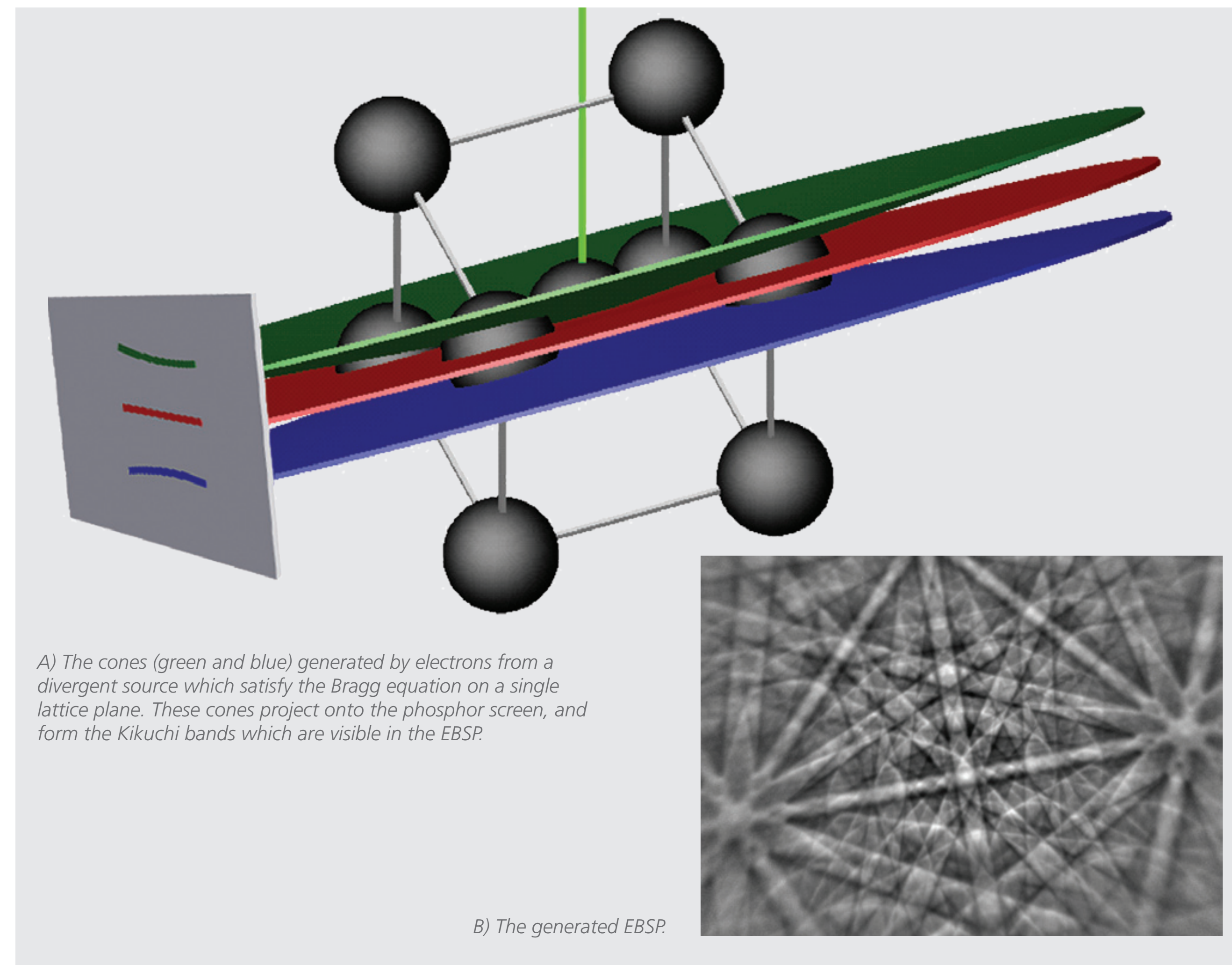

Fig. 2. The formation of the electron backscattered diffraction pattern (EBSP).

Band intensity

The mechanisms giving rise to the Kikuchi band intensities and profile shapes are complex. As an approximation, the intensity of a Kikuchi band for the plane (hkl) is given by:

$$I_{hkl} = \left[\sum_i f_i(\theta)cos2\pi(hx_i + ky_i + lz_i)\right]^2 + \left[\sum_i f_i(\theta)sin2\pi(hx_i + ky_i + lz_i)\right]^2$$

where $f_i(\theta)$ is the atomic scattering factor for electrons and (x_i y_i z_i) are the fractional coordinates in the unit cell for atom i. A collected diffraction pattern should be compared with a simulated pattern calculated using the previous equation. This ensures only planes that produce visible Kikuchi bands are used when solving the diffraction pattern. The optimum number of reflectors to use depends on the phases that the system needs to distinguish between, and on the crystal symmetry of the phases.

Interpreting the diffraction pattern

The centre lines of the Kikuchi bands correspond to where the diffracting planes intersect with the phosphor screen. Hence, each Kikuchi band can be indexed by the Miller indices of the diffracting crystal plane which formed it. The intersections of the Kikuchi bands correspond to zone axes in the crystal. The semi-angle of the diffracted cones of electrons is $(90-\theta)°$. For EBSD, this is a large angle so the Kikuchi bands approximate to straight lines. For example, the wavelength of 20 kV electrons is 0.00859 nm and the spacing of the (111) plane in Aluminium is 0.233 nm, making the cone semi-angle 88.9°.

The width w of the Kikuchi bands close to the pattern centre is given by:

$$w \approx 2l\theta \approx \frac{nl\lambda}{d}$$

where l is the distance from the sample to the screen. Hence, planes with wide d-spacings give thinner Kikuchi bands than narrow planes. Because the diffraction pattern is bound to the crystal structure of the sample, as the crystal orientation changes, the resultant diffraction pattern also changes. The positions of the Kikuchi bands can therefore be used to calculate the orientation of the diffracting crystal (Fig. 3).

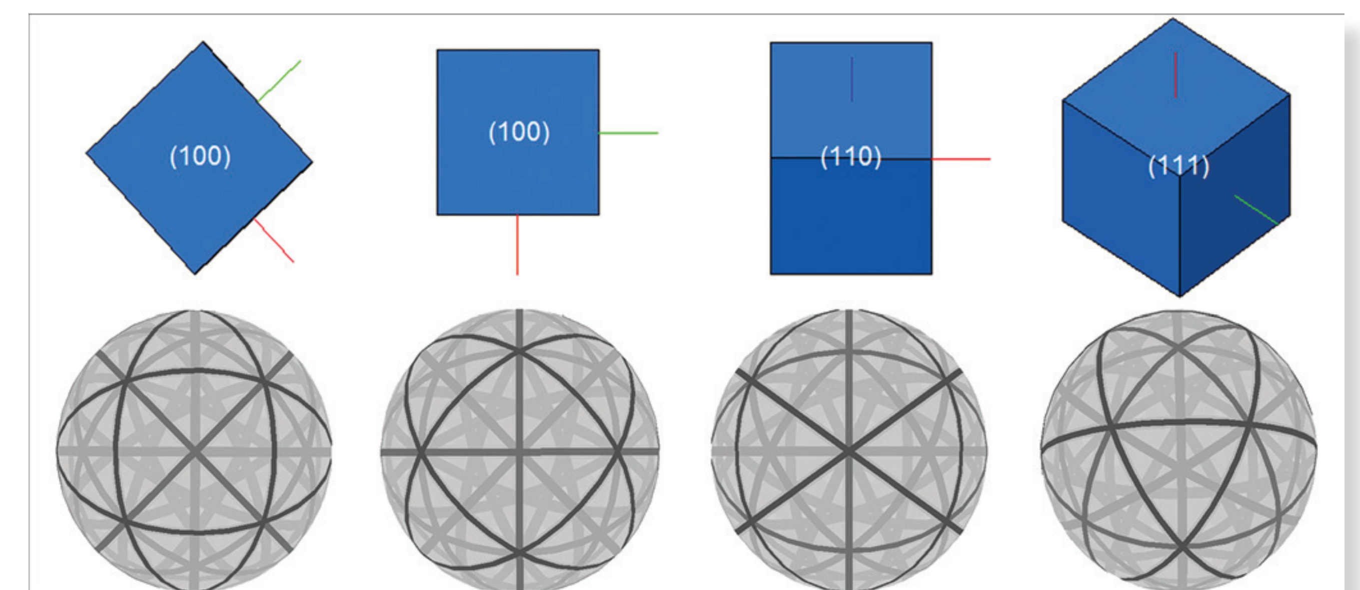

Fig. 3. The spherical diffraction patterns generated by different orientations of a cubic structure.

Basics of EBSD...

Calibrating an EBSD system

In order for an EBSD system to work correctly, it must first be calibrated. Typically, the EBSD system calibration involves measuring the sample-to-screen distance and the pattern-centre position on the phosphor screen. The pattern centre is the point on the screen closest to the generation point of the diffraction pattern on the sample.

There are several methods for calibrating an EBSD system. The preferred method is to collect diffraction patterns from the same point on a sample with the detector placed at different insertion positions (Fig. 4).

Using image correlation, it is then possible to identify the pattern centre.

In a modern EBSD system the calibration is automated, so the system can be used seamlessly at any geometry and by any user.

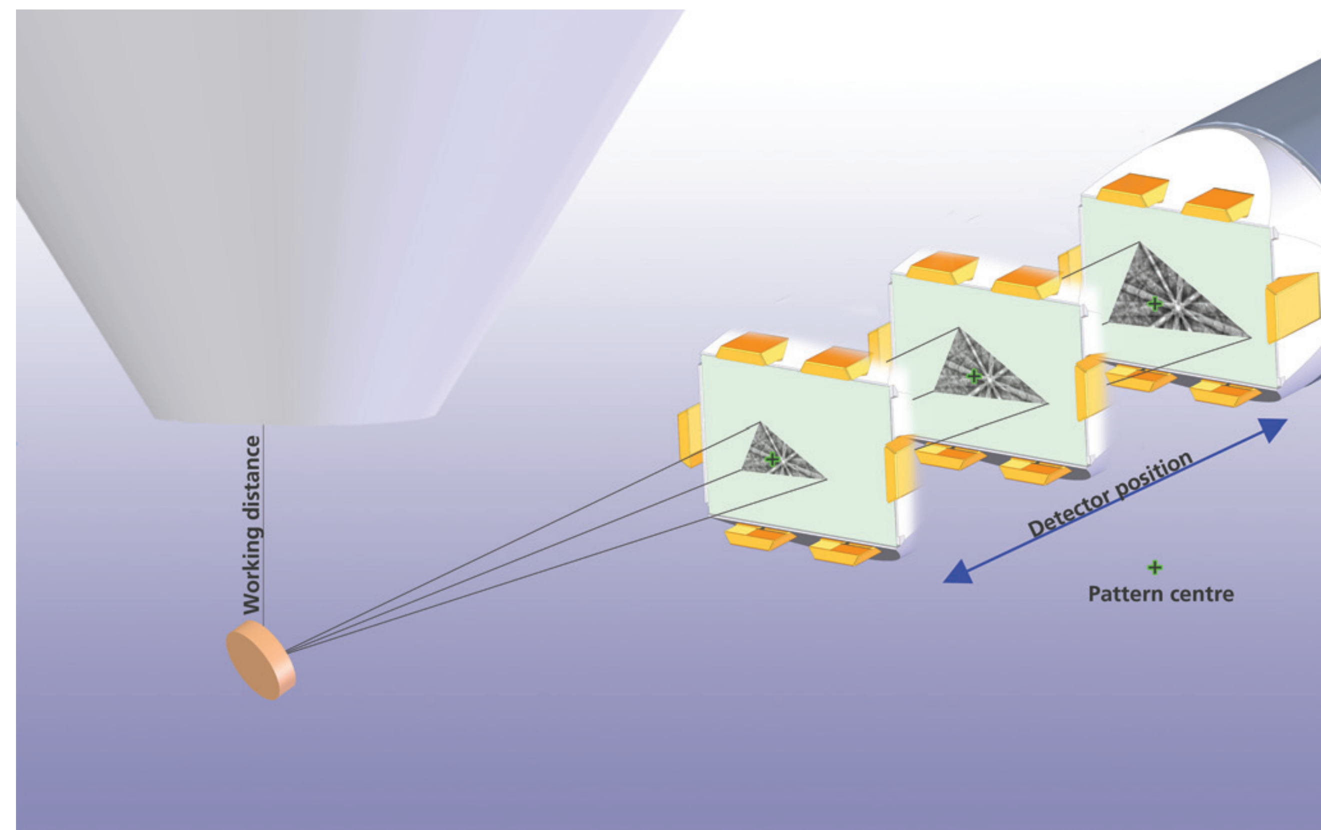

Fig. 4. The pattern centre is found by correlating features on the EBSPs at different detector positions. The pattern centre is the zoom point on those EBSPs - the one point which does not move when the detector moves.

Basics of automated indexing

Once an EBSD system has been calibrated, it becomes possible to automatically index the diffraction patterns and calculate the crystal orientation. This is typically accomplished using the following steps:

1. The diffraction pattern is transferred from the camera inside the detector to the EBSD software.
2. The Hough transform is used to calculate the positions of the Kikuchi bands.
3. Having identified the Kikuchi band positions and from knowing the calibrated geometry, it is possible to calculate the angles between the detected bands.
4. The calculated angles are compared with a list of interplanar angles for the analysed structure(s).
5. The possible solutions are sorted to find the best fit and the orientation matrix is calculated.

This whole process is automatic and takes less than a few milliseconds on modern computers.

The Hough transform

The Hough transform, which is used to identify the positions of the Kikuchi bands, converts the image from the EBSD camera into a representation in Hough space, by using the following relation between the points (x, y) in the diffraction pattern and the coordinates (ρ, θ) of the Hough space:

$$\rho = x\cos\theta + y\sin\theta$$

A straight line in the image space (x, y) can be characterised by ρ, the perpendicular distance from the line to origin and θ, the angle made with the x-axis, and can be presented by a single point (ρ, θ) in Hough space (Fig. 5). The Kikuchi bands appear as bright regions or peaks in Hough space, which are easily detected and used to calculate the original band positions (Fig. 6).

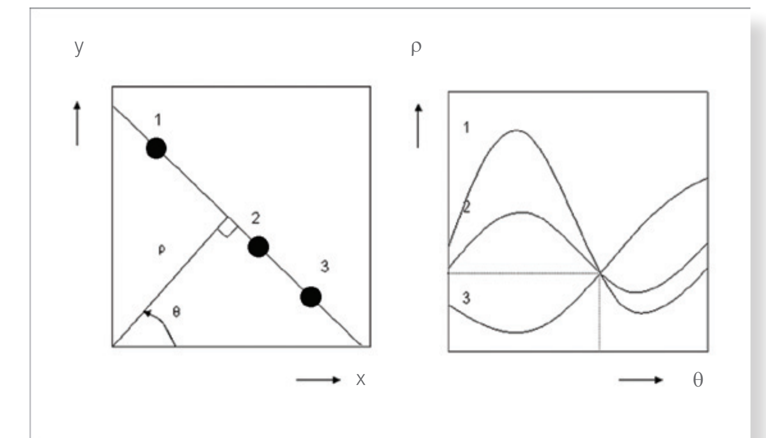

Fig. 5. The Hough transform converts lines into points in Hough space.

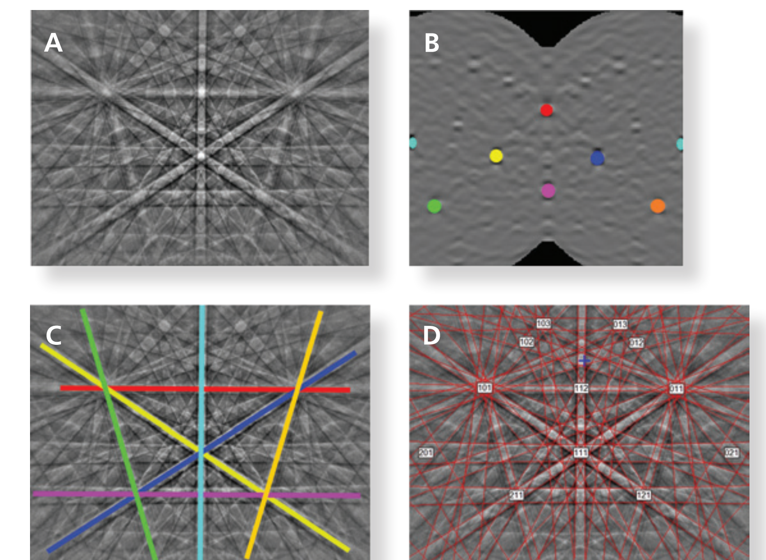

Fig. 6. Finding the position of the Kikuchi bands in the diffraction pattern using the Hough transform.

A) Diffraction pattern collected from silicon at 20kV accelerating voltage;

B) The peaks in the Hough transform identified and coloured;

C) The bands in the original diffraction pattern corresponding to the peaks found in the Hough transform and coloured similarly;

D) The indexed diffraction pattern with the blue cross indicating the position of the pattern centre.

EBSD Developments

Band detection

Band detection is a fundamentally important aspect of EBSD and is critical in terms of data quality. Improvements in band detection can increase the number of correctly indexed points, especially for materials that exhibit indistinct bands or have low quality patterns, such as those consisting of highly strained or partially recovered microstructures.

The band detection in modern systems uses a sophisticated algorithm which automatically determines which of the detected bands are best used in the indexing. This method applies a weighting function based on the band's average intensity and the position of the band within the area of interest - the area of the EBSP used for band detection. Higher priority is given to those bands at or near the centre of the area of interest, and therefore bands which are more reliably detected are used in the indexing, thus making the indexing more robust.

However, in reality neither pattern nor band detection are always perfect. Pattern quality may be poor, patterns may be overlapping, bands will be missed, and so indexing needs to be robust.

Indexing routines

The indexing routine is critical to achieve accurate data. The challenge is to achieve a high validated hit rate without generating false positive solutions, where EBSPs are solved but with the wrong solution. In addition, automated routines can be very sensitive to non-fitting bands, such as those that might occur at a grain boundary. Therefore, the algorithm applied in the indexing must be robust enough to handle inaccuracies in band detection and identify the correct solution.

A method called "Class Indexing" examines permutations of four bands, and considers band coherence (where the measured bands and reference crystal reflectors are in agreement) and non-coherence (where the measured bands and the reference crystal reflectors are not in agreement). These four-band combinations enable the indexing routine to break the solutions into smaller blocks, which are then the foundations of the indexing. Using this method, the routine is far more robust and can find the correct solution even when one or more bands are non-coherent.

There have traditionally always been difficulties when using EBSD to distinguish phases with similar crystal structures because the technique generally uses only the angles between the bands to identify the phase. One technique that can aid in these situations is to use the difference in lattice parameter (or band width). If sufficient, it is possible to use the difference in the band widths to distinguish these phases.

An alternative is to combine the EBSD indexing routine with input information based on the sample chemistry, by simultaneously collecting EDS (Energy Dispersive Spectrometry) and EBSD data, for example through the **AZtec** TruPhase routine (Fig. 7). This can be used when both EDS and EBSD are suitably setup on the SEM, allowing both to work in the same geometry at the same time. The TruPhase routine correlates the measured spectra acquired during mapping against predefined spectra for the phases of interest.

Refined accuracy

Correct identification of orientation relies on accurate detection of band positions and therefore indexing. When highest precision misorientation measurements are required (e.g. characterisation of subtle sub-grain structures), the Refined Accuracy* mode in **AZtec** can be used. It significantly improves on the precision of misorientation measurement compared to conventional (Hough-based) methods, without dramatically affecting speed.

After a primary, Hough-based band detection, Refined Accuracy employs a secondary band refinement, which fits the simulated band to the actual band in the EBSP itself (taking into consideration the profile of the band edges). The band position (parameters ρ and θ) is thus more accurately determined, leading to better precision in orientation measurement.

* patent pending

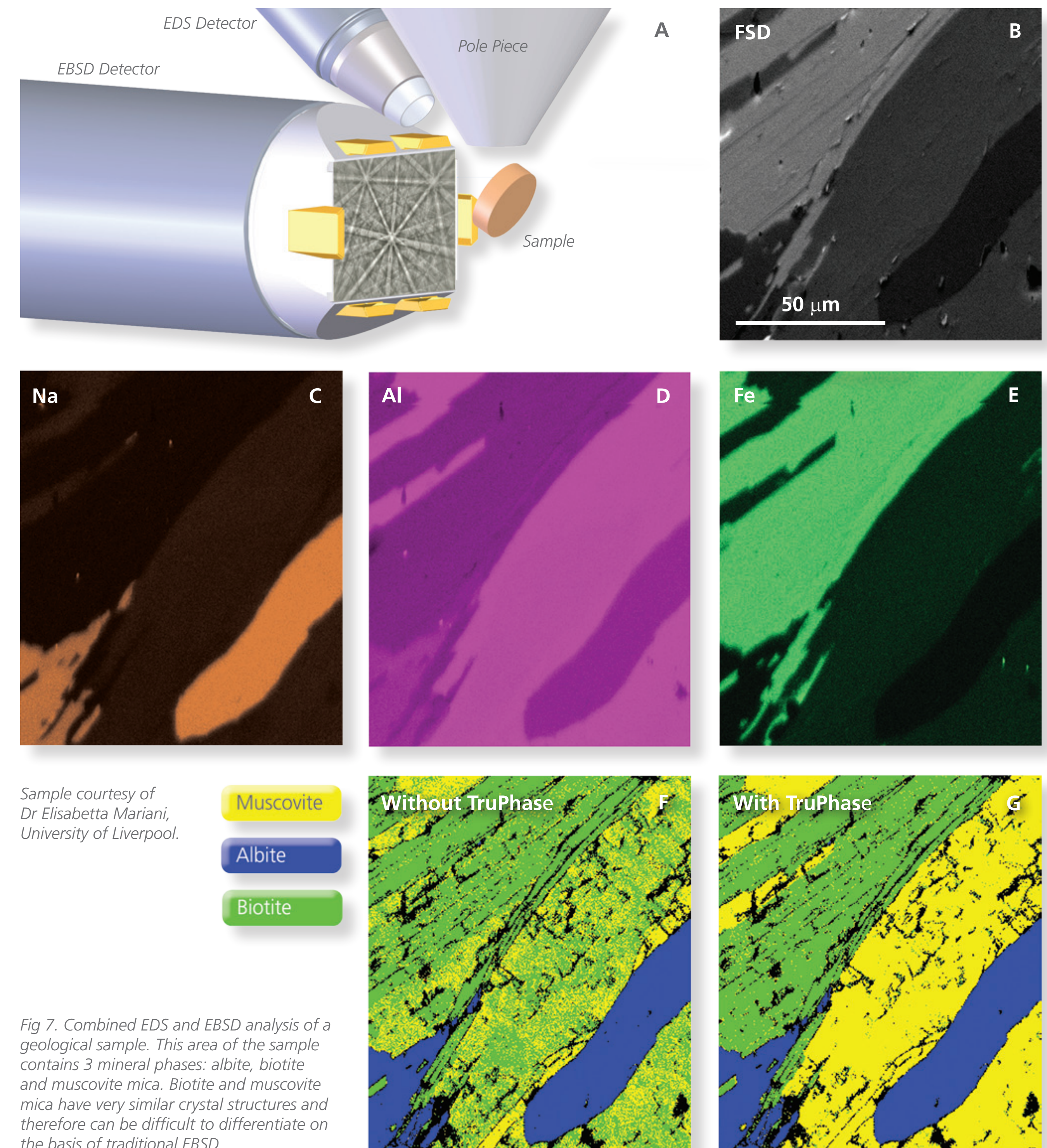

Sample courtesy of Dr Elisabetta Mariani, University of Liverpool.

Fig 7. Combined EDS and EBSD analysis of a geological sample. This area of the sample contains 3 mineral phases: albite, biotite and muscovite mica. Biotite and muscovite mica have very similar crystal structures and therefore can be difficult to differentiate on the basis of traditional EBSD.

A) The relative positioning of the sample, EDS and EBSD detectors inside the SEM chamber.
B) A forescatter diode (FSD) image of the area of the sample being analysed.
C) Na element map, the highest concentration is found in albite.
D) Al element map, the highest concentration is found in muscovite.
E) Fe element map, the highest concentration is found in biotite.
F) A phase map acquired using traditional EBSD. Due to their similar crystal structures, biotite and muscovite are poorly differentiated, resulting in a speckled appearance.
*G) A phase map acquired using the TruPhase routine in **AZtec** where EDS data is collected simultaneously to EBSD data and used to inform the solution given for the EBSP. This method successfully differentiates the biotite and muscovite mica in the sample.*

EBSD Data acquisition

A common first step in characterising a sample is to overview the microstructure and identify regions of interest for further analysis. On an SEM, this normally means using the SE (secondary electron) or BSE (backscatter electron) detectors to generate images.

When working with samples in the tilted geometry, it is not always possible to use the BSE detector, and the SE detector is not always in the ideal geometry. This means that the signal for both these detectors might be compromised. To optimise imaging at this geometry EBSD detectors often have FSD diodes fitted above and below the phosphor screen.

Forescatter diodes (FSD)

FSD diodes can be used for imaging, and, due to their position around the EBSD detector, they detect electrons that have interacted with the sample in different ways. This leads to different contrast mechanisms and different images (Fig. 8). The upper diodes primarily detect backscatter electrons (large-angle scattering), which means that the images generated by the upper diodes are dominated by atomic-number contrast, hence revealing variations in chemistry. The lower diodes primarily detect electrons that have gone through a low-angle scattering coming from the interaction with the lattice, leading to images generated based on orientation contrast.

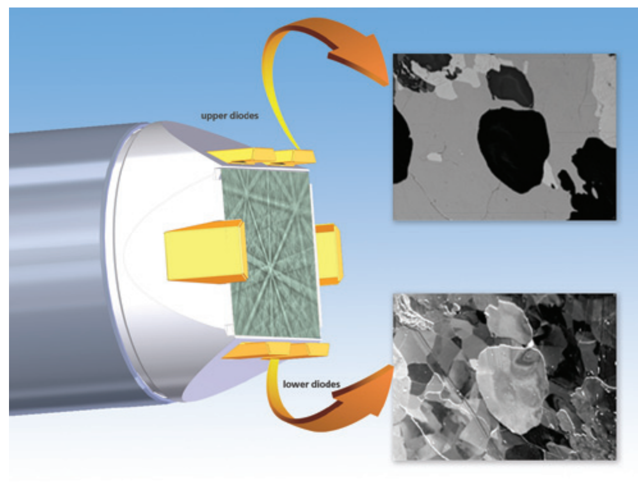

Fig. 8. The positioning of the forescatter diodes and examples of the images collected from a geological sample by the upper and lower diodes.

PhaseID

In order for an EBSD system to index an EBSP, it needs to know which phase(s) to index against. Therefore the first step of the analysis is to identify the phases that are present in the sample.

If the EBSD system is not integrated with an EDS system, the user must know beforehand what phases are present in the sample, either from EDS analysis undertaken independently or from the history of the sample. Using this knowledge, the user can generate a list of possible phases. However, the list might not be complete or it might contain phases that are not actually in the sample. To check which phases are present, the FSD image is a useful reference for collecting reference EBSPs from the different areas and checking those EBSPs against the manually generated list of phases.

If the EBSD and EDS systems are integrated and installed in a suitable geometry on the SEM, it is possible to use the FSD image as a reference, and place the beam on each of the potential phases to acquire an EBSP and an EDS spectrum at the same time. For each beam position, the system can search available crystal structure databases for entries that match the chemistry of the phase, as determined from the obtained EDS spectrum. These candidate phases will then be used for indexing the collected EBSP, and the outcome is that the system identifies the structure based on both chemical and crystallographic information.

It is also possible to use chemical element maps as a reference. However, it is often better to use the FSD images because they contain information about the grain structure, which makes it possible to identify smaller particles, and helps to ensure that the beam is placed within a grain and not on a boundary.

Phase discrimination

The detected Kikuchi pattern is generated by the electron beam interacting with the crystal structure in the surface layer of the sample. This means that the EBSP carries information about the crystal structure it was generated from. By analysing the EBSP, we can get information not just about the orientation of the crystal but also information that makes it possible to distinguish between different crystal structures, and hence phases. An example is shown in Fig. 9.

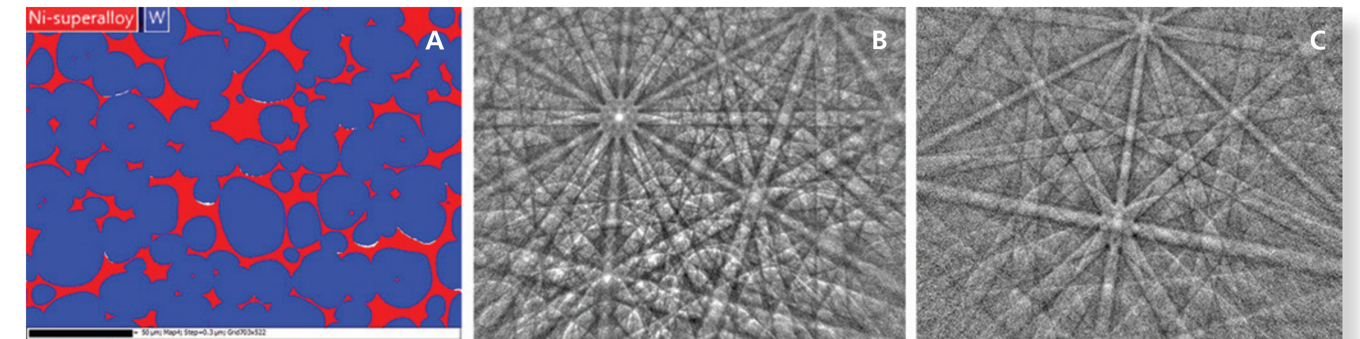

Fig. 9. The discrimination of the two phases present in a sample of tungsten hardened alloy. A) A phase map showing the two separate phases (Ni is shown in red and W in blue). B) A typical EBSP obtained for W. C) A typical EBSP for Ni.

Typically EBSPs are analysed by looking at the angles between the detected bands. If only this information is used, then it is possible to distinguish between phases that have different unit cell structures as long as one structure is not just a scaling of another (Fig. 10).

Modern systems can extract information about the width of the bands within the EBSPs, which helps to distinguish between phases of same structure type but different lattice parameters.

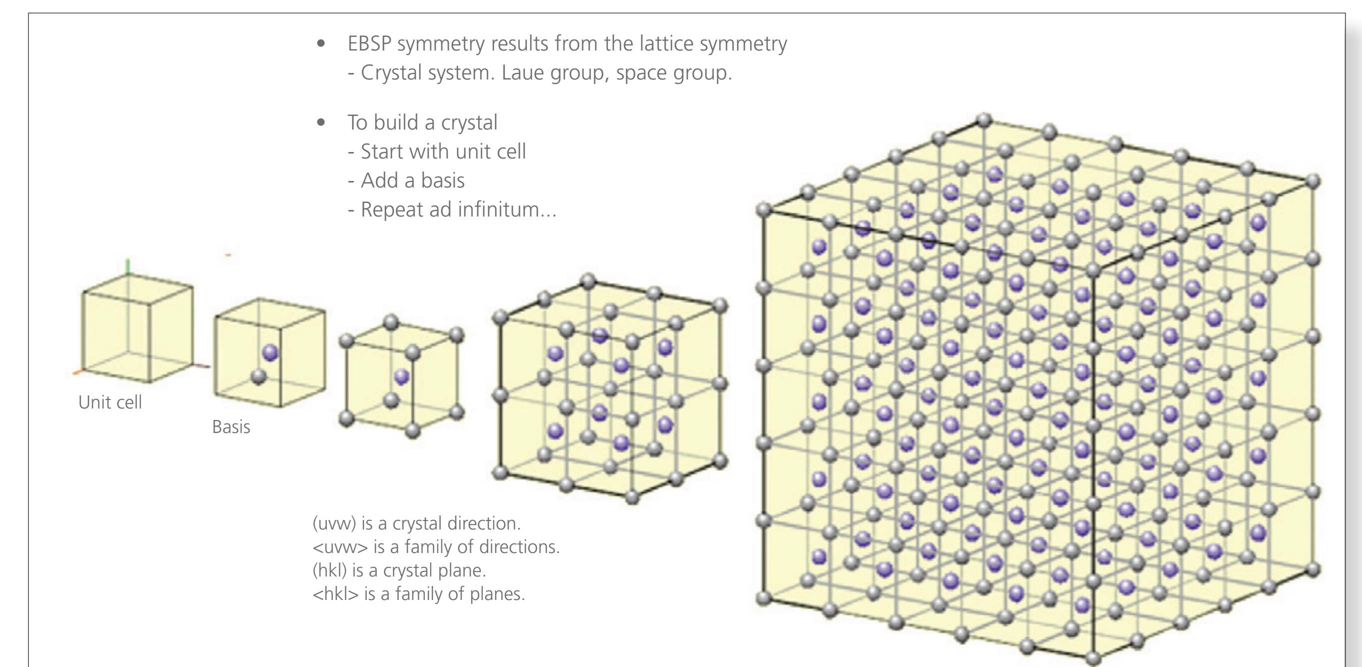

Fig. 10. The scaling of unit cell structures.

EBSD Data acquisition...

Point analysis

It is important to check that the EBSPs are of a reasonable quality before starting to collect data from a sample (e.g. a map). If the EBSPs look reasonable, the next step is to check the band detection settings and that the EBSP can be successfully indexed based on the phases in the phase list. By manually repeating these steps at different beam positions, it is also possible to get a quick overview of the microstructure.

An example is shown (Fig. 11) where point analysis is used to acquire data and determine the orientation in a few selected grains, which could be all the data collection required if there are only a few grains of interest within the sample.

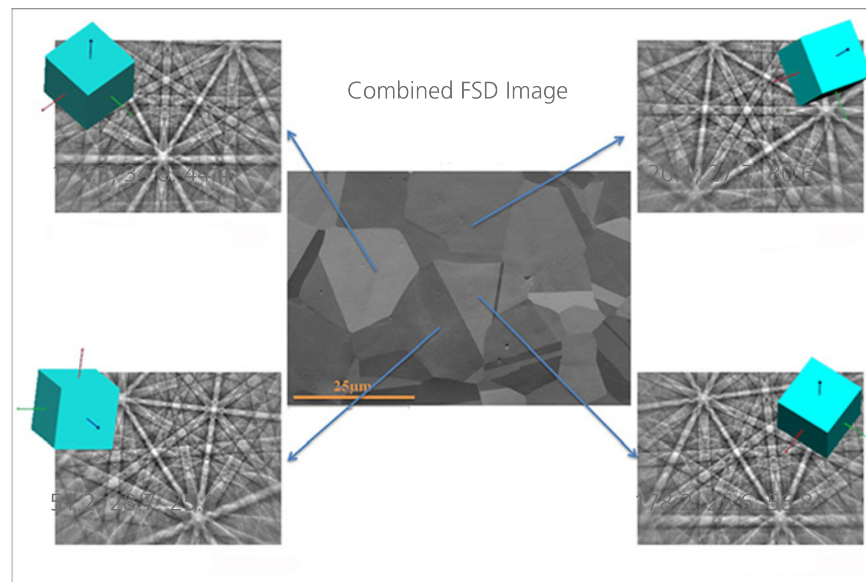

Fig. 11. Point analysis of grains in steel showing the diffraction pattern generated and the calculated crystal orientation in Euler Angles.

Mapping

The typical sequence for manual point analysis is:

1. Position beam
2. Acquire EBSP
3. Detect bands
4. Index based on phase list
5. Save the result. At each beam position, the system typically saves:
   - Pattern quality values calculated based on the EBSP
   - Phase information
   - Orientation
   - Euler angles
   - MAD (Mean Angular Deviation) as a measure of the fit between EBSP and solution
   - EDS data, if the EBSD and EDS systems are integrated

When all the parameters have been setup, such that no further user intervention is required, this flow can be automated to cover a large area of the sample. During mapping of the sample, the above sequence is carried out for each beam position as the beam automatically moves across the sample surface.

Typical data presentations

PhaseMap

Based on the saved information, it is possible to generate different map displays. For example, it is easy to generate a map showing how the phases are distributed within the sample. This can be done by assigning a colour to each phase, and colouring the map pixel based on which phase was found during the analysis (e.g. Fig. 9).

Pattern quality map

Pattern quality values are typically calculated based on the intensity of the peaks (or peak profile) in the Hough space, one way of calculating a pattern quality parameter p would be:

$$p = \sum_{i=1-3} h_i / 3\sigma_h$$

where h_i is the peak height of the Hough transform of the i'th most intense Kikuchi band, and σ_h is the standard deviation of the Hough transform, however it is normally calculated in a more advanced way. The pattern quality parameter will associate a number with how sharp or well defined the band positions are in the EBSP. This means that the pattern quality (e.g. Fig. 12) will be influenced by several factors: phases, orientation, contamination, sample preparation and the local crystalline perfection.

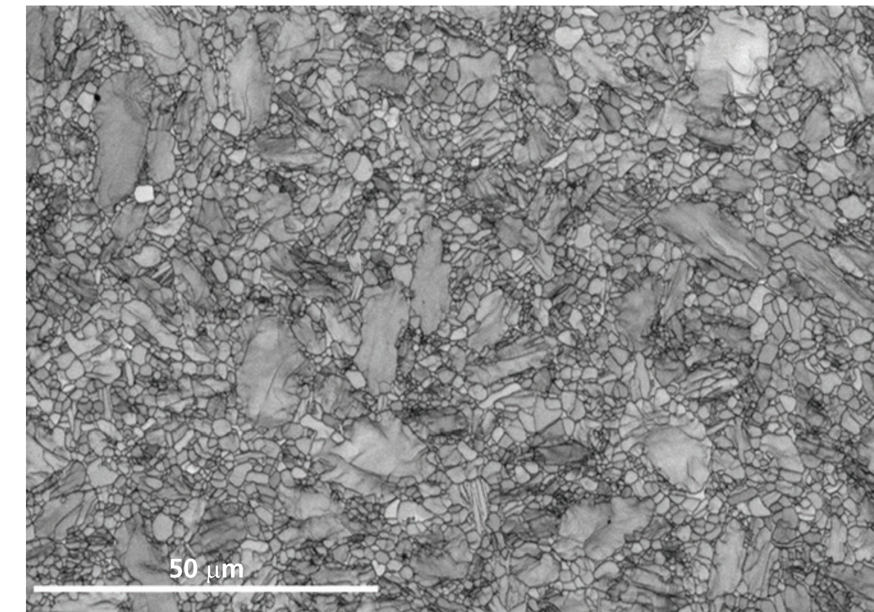

Fig. 12. A pattern quality map for a sample of Ti64. Dark areas are indicative of poorer pattern quality and light areas of higher pattern quality.

Pattern quality maps will often reveal features invisible in the electron image such as grains, grain boundaries, internal grain structure and surface damage such as scratches. This makes the pattern quality map very useful during the analysis of the data but also as a simple tool for checking if the sample stayed in focus during the data collection or if the sample drifted.

Typical data presentations...

Euler angles

The determined orientations are normally described by a set of Euler angles. Euler angles are the most commonly used way to describe the sample orientation relative to the crystal, where each crystal structure has been given a certain reference orientation. This involves rotating one of the coordinate systems about various axes until it comes into coincidence with the other. There are several conventions on how the rotations are to take place. The most commonly used way is to use the Bunge notation where the three Euler angles: (phi1, phi, phi2) represent the following rotations, which are shown schematically in Fig. 13:

1. rotation of phi1 about the z-axis followed by,
2. rotation of phi about the rotated x-axis followed by,
3. rotation of phi2 about the rotated z-axis

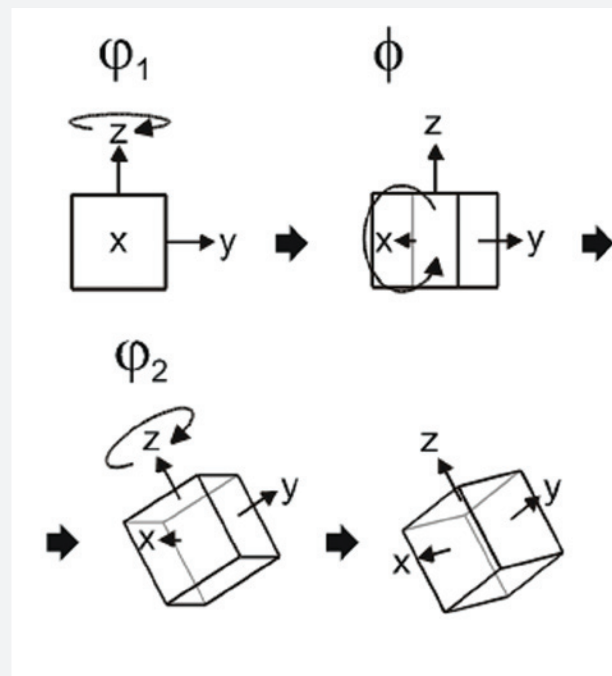

Fig. 13. Euler angles and rotations.

Orientation maps

The simplest way of generating an orientation map is by plotting the 3 Euler angles using an RGB colour scheme; this is often referred to as an Euler map (Fig. 14).

The Euler coloured maps give a basic presentation of the microstructure. However there are limitations of the Euler maps. One of the issues is that small orientation changes don't always correspond to small changes on the colour scale, which can cause confusion when looking at an Euler map.

To accommodate these issues, a different type of map display is often used. The Inverse Pole Figure (IPF) colour scheme uses a different colour scheme, which is...

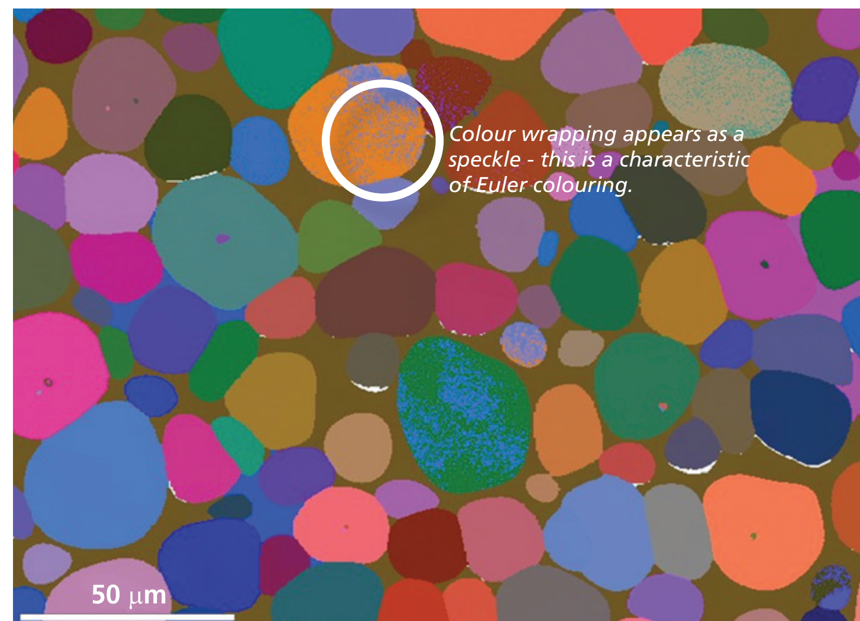

Fig. 14. An all Euler angle colouring orientation map for the sample of tungsten hardened alloy shown in Fig. 9. Note the colour wrapping that is characteristic of Euler colouring.

...much easier to interpret and which normally doesn't have large colour changes when there are small changes in orientation. The colour scheme is designed by assigning a colour to each of the corners of the inverse pole figure (Fig. 15). For each map, a reference sample direction (like rolling direction) is chosen, and the colour is assigned based on the measured crystal orientation and the chosen viewing direction.

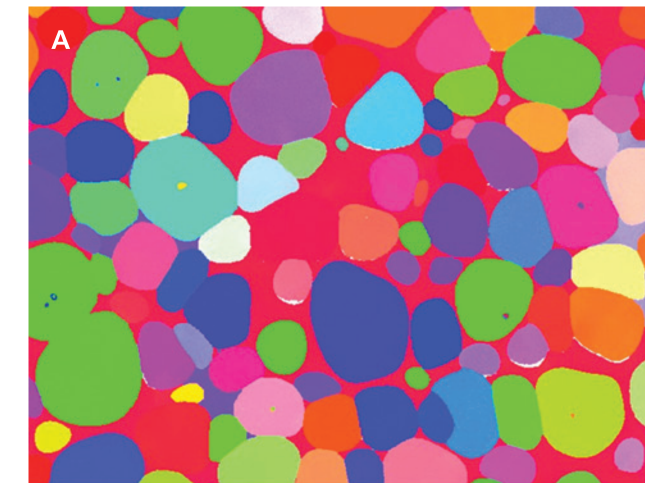

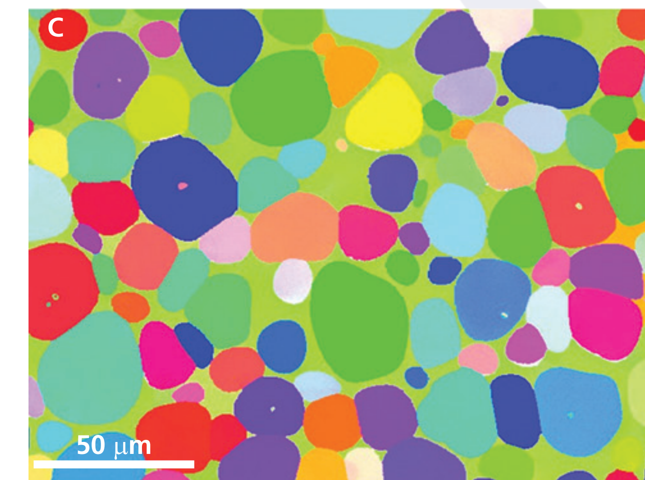

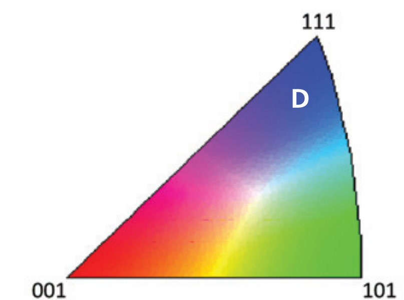

Fig. 15. Crystal orientation maps obtained for a sample of tungsten hardened alloy (shown in Figs. 8 and 14) collected at 20 kV accelerating voltage.

A) X direction IPF colouring orientation map;

B) Y direction IPF colouring orientation map;

C) Z direction IPF colouring orientation map;

D) IPF colour key.

Typical data presentations...

Misorientations

EBSD has a significant advantage over many other microstructural characterisation techniques in that it can measure the misorientation between two crystals (i.e. the difference in the orientation). In order to define a misorientation, it is easiest to consider a triclinic crystal – i.e. one that has no symmetry. For any two triclinic crystals, there is a unique rotation axis and rotation angle which maps one crystal lattice onto the other. These are referred to as the Misorientation Axis and the Misorientation Angle.

When the crystals in question have some symmetry, then there is no longer a unique axis-angle pair that describes the misorientation between 2 crystal lattices. Depending on the symmetry, there may be up to 24 symmetrically equivalent axis-angle pairs that match 2 crystal lattices. It is not possible to determine which of these different solutions is correct, and therefore it is convention to take the solution that has the lowest misorientation angle (also referred to as the disorientation angle).

Grains and grain boundaries

A grain is a three-dimensional crystalline volume within a sample that differs in crystallographic orientation from its surroundings but internally has little variation. To identify the grains within a dataset, it is required to define a critical misorientation angle where all boundary segments with an angle higher than the defined critical angle are to be considered grain boundaries. By measuring the misorientation between all pixel pairs, it is possible to identify the boundaries enclosing the individual grains. If this information is used together with the phase information, then it becomes possible to determine the grain size distributions from different phases within the sample.

In a similar way, generating a map that shows the spatial distribution of the grain boundaries can often provide additional information about the microstructure. A typical example would be to generate a map showing low-angle boundaries (which can give information about substructure of individual grains) together with high-angle boundaries (which define the grain structure), Fig. 16.

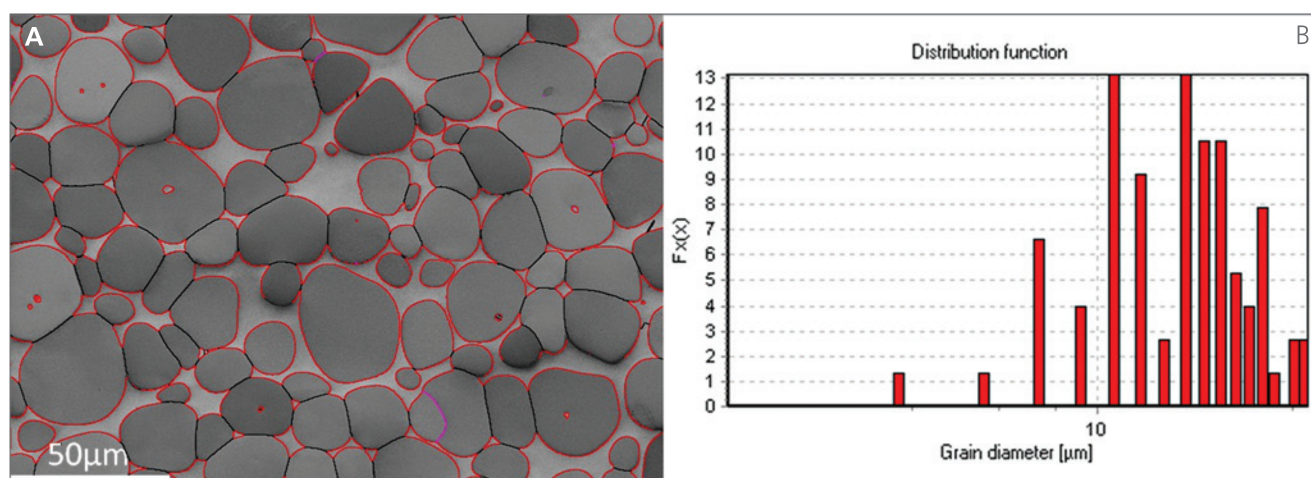

Fig. 16. Grain boundary data for a sample of tungsten hardened alloy (shown in Fig. 9).

A) Grain boundary positions superimposed on the pattern quality image with grain boundaries higher than 2 degrees highlighted in purple, higher than 10 degrees in black, and phase boundaries are in red;

B) Histogram of grain sizes from the Tungsten (W) phase. The average grain size is shown to be 17 µm.

When the misorientation angle is calculated, it is also possible to calculate the misorientation axis, as mentioned earlier. This means that EBSD data can be used to identify specific or special boundaries defined not just by a misorientation angle but by a combination of misorientation angle and misorientation axis. The most common example would be twin boundaries, which are a subset of the coincident site lattice (CSL) boundaries. CSL boundaries are special boundaries that fulfil the coincident site lattice criteria whereby the lattices are sharing some of the lattice sites. CSLs are characterised by Σ, where Σ is the ratio of the CSL unit cell compared to the standard unit cell. Two examples of CSL relationships are shown in Fig. 17.

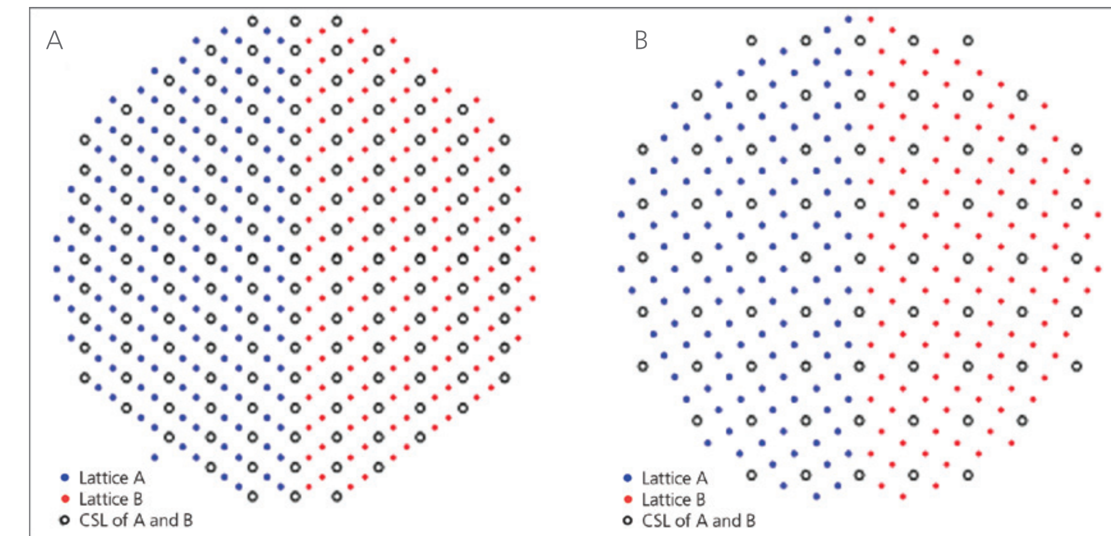

Fig.17. A) The sigma 3 boundary (twin boundary) is a 60° rotation about the [111] direction. B) The sigma 5 boundary is a 36.9° rotation about the [100] direction.

CSL boundaries typically have a significant impact on the material properties, which means that from a materials engineering viewpoint it becomes important to determine the ration of CSL boundaries and their distribution within the material. An example from twinned nickel is in Fig. 18. As shown on the CSL histogram, the Σ3 boundary is the most frequently occurring CSL boundary, which is also shown on the map where all the Σ3 (60°, [111]) boundaries are coloured red.

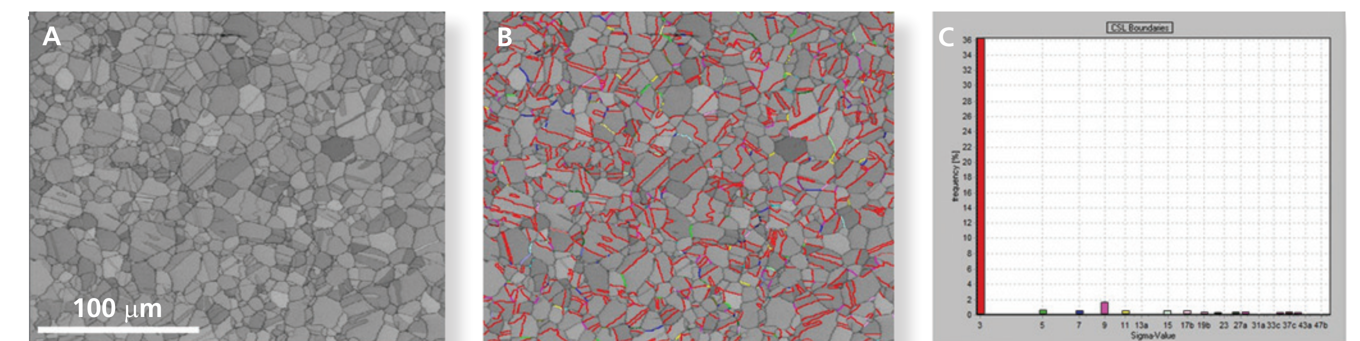

Fig. 18. CSL boundary data measured by EBSD for a Nickel sample.

A) Pattern quality map for a sample of Nickel;

B) Coincident site lattice (CSL) boundary positions superimposed on the previous pattern quality image;

C) The boundaries are colour coded by CSL type as shown in the histogram of CSL found.

In most materials, grains do not have a completely random orientation distribution, and when the distribution is not random, the sample is said to have a preferred orientation or texture. Based on the orientation information acquired from several points within each phase, it is possible to statistically check whether a given phase has a preferred orientation. This can be done in several ways; one way would be to look at maps highlighting the points with an orientation close to a specified reference orientation, referred to as texture maps. They can be very useful because they contain information about the spatial distribution of the reference texture (Fig. 19).

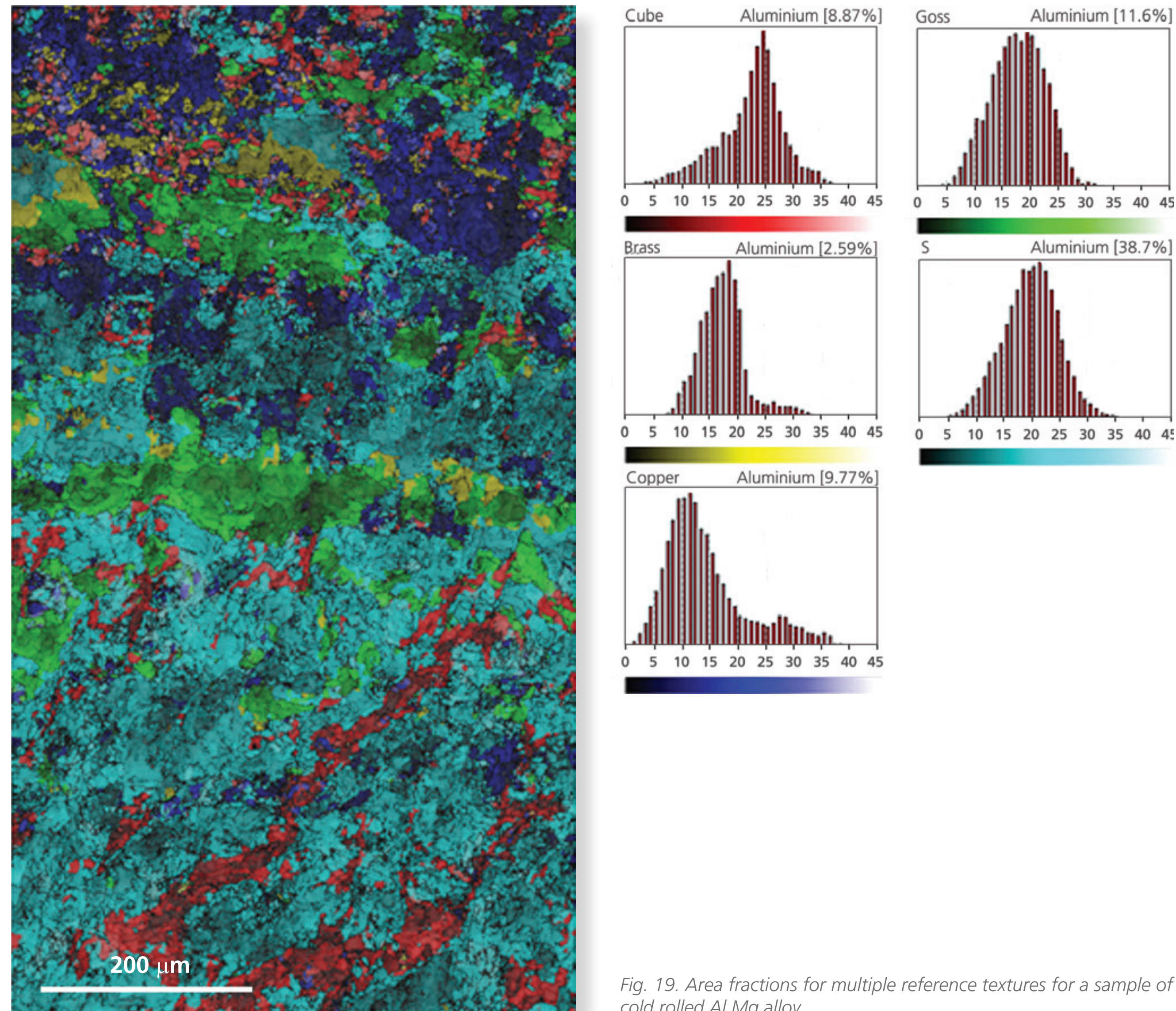

Fig. 19. Area fractions for multiple reference textures for a sample of cold rolled Al Mg alloy.

Another approach is to generate pole figures for the identified phases, and to use the pole figures to reveal information about the texture within a given phase. If there are several phases within the sample, pole figures can easily be used to identify relationships between the orientations near the interface boundaries (Fig. 20).

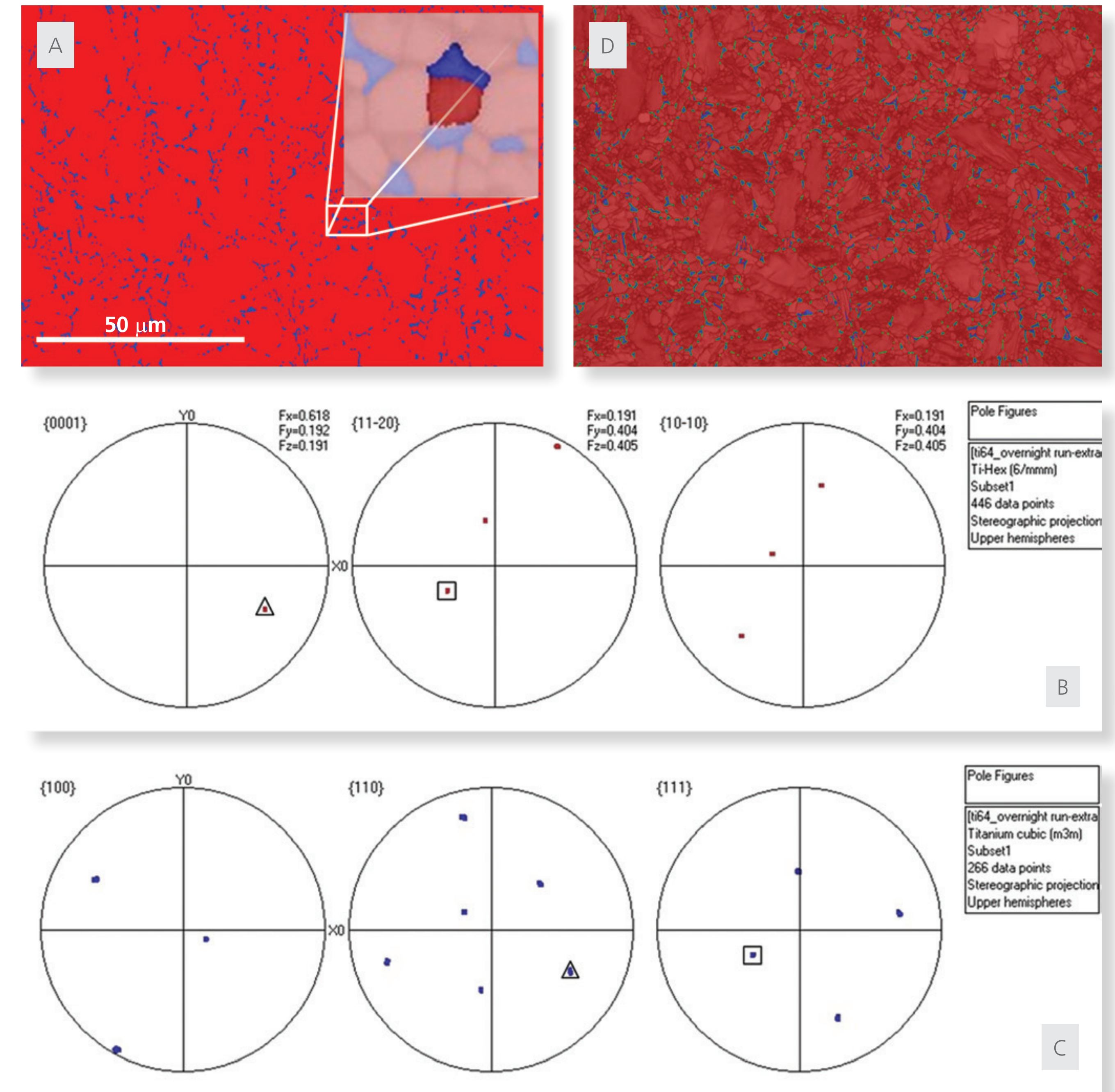

Fig. 20. Orientation relationship between Ti alpha and Ti beta.

A) Phase map of Ti 64 shows the phase distribution and one grain from each phase selected for further analysis; Ti alpha is red and Ti beta blue.

B) Pole figures from the selected Ti alpha grain.

C) Pole figures from the selected Ti beta grain.

D) Phase map plus band contrast and grain boundaries with Burgers orientation relationship {0001}//{011} and <2-1-10>//<11-1> in green.

Typical data presentations...

Pole figures

Pole figures are tools for plotting 3D orientation information in 2D (such as on a sheet of paper or a computer screen). They are useful for showing the orientations of specific crystallographic planes and directions within a sample (i.e. for plotting the texture) and, as such, are invaluable for EBSD.

A pole figure shows the projected position of a particular set of crystallographic planes, where the "poles" (or normals) have been projected onto a sphere and then onto a circle. There are two main methods for doing this, the stereographic and equal area projection. This section explains the stereographic projection.

If we start with a single crystal, shown by the unit cell on the left in Fig. 21, it is orientated in a particular manner relative to the sample, bottom left of Fig. 21.

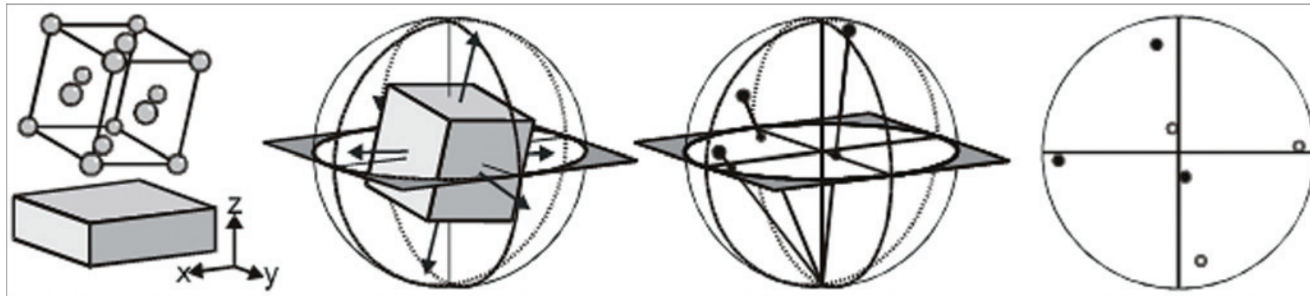

Fig. 21. The production of a stereographic projection for a single crystal (in this case a unit cell), which is orientated in a particular manner to the sample.

The {100} plane normals, of which there are 6 for this cubic crystal, would project onto a sphere as shown in the second drawing. A plane, parallel to the sample surface and passing through the centre of our sphere would intersect the sphere as a circle.

We now join the points where the {100} plane normals touch the sphere to the sphere's opposite pole. This is shown in the third image. Note: only the upper hemisphere points are shown. It is possible to repeat the process for the lower hemisphere points. In general, in materials science, it is conventional to plot in the upper hemisphere, whereas in the Earth sciences the lower hemispheres are commonly used.

If we now look at just the circle, we will see that the three-dimensional crystallographic directions have been converted into points. This is the {100} pole figure. This can be repeated with the orientations of other grains to give a pole figure that shows the distribution of that particular set of planes within the sample. If there is a tendency for the points to be arranged in a particular manner, then we have a texture.

Inverse pole figures

A pole figure plots crystallographic directions in the sample coordinate system, whereas an inverse pole figure plots sample directions in the crystallographic coordinate system. For example, instead of plotting the <111> directions in terms of the rolling direction (RD) and normal direction (ND), an inverse pole figure could plot the rolling direction in terms of the major crystal directions (i.e. [100], [110] and [111]). Inverse pole figures have several benefits over conventional pole figures, such as:

- Each data point appears as a single point in an inverse pole figure. In many pole figures, for higher symmetry phases, a single data point may be represented by multiple points on the pole figure (e.g. 3 symmetrically equivalent {100} poles).
- It is often easier to pick out particular fibre textures using an inverse pole figure.
- Inverse pole figures are often used as a default colouring scheme for orientation maps (by colouring the three corners of the inverse pole figure triangle with the primary colours).

The appearance of an inverse pole figure depends on the Laue group of the relevant phase. This determines the size of the "unit triangle" – i.e. the symmetrically equivalent space in the whole stereographic projection. For example, a triclinic crystal (Laue group 1) has no symmetry and therefore the whole pole figure is necessary to show all the possible crystal directions. Therefore for triclinic structures, the inverse pole figure is like a pole figure – a full circle.

As the symmetry of the structure increases, the size of the symmetrically equivalent region decreases until, for Laue group 11 (cubic high), there are 24 symmetrically equivalent regions in the full circle. This is shown in Fig. 22, with the standard unit triangle highlighted in the IPF colouring scheme.

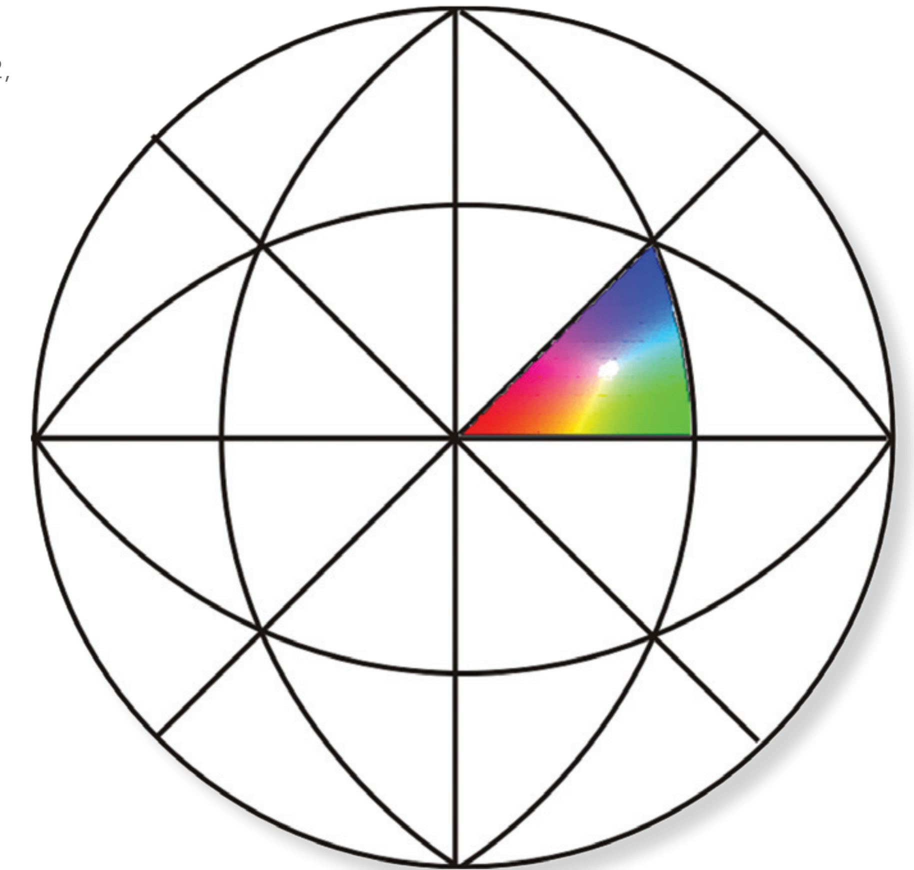

Fig. 22. The 24 symmetrically equivalent regions in the (high) cubic inverse pole figure.

3D EBSD

As shown by different examples, EBSD can provide information from the sample surface. However, there is often a requirement to get the same type of information from a 3D volume to study grain structures, grain size and interface boundaries. Depending on the dimensions of the volume of interest, this can be achieved in several ways. For large scale features, it is possible to use mechanical sectioning techniques to expose a new surface at different depths of the sample. For small scale features, it is not practical to take the sample out of the SEM chamber and then reposition it to collect more data. One solution is to use an SEM combined with a focused ion beam (FIB-SEM), where the ion column can be used to mill away the surface between each EBSD map.

To automate this process, the sample must be placed in a geometry suitable for milling, with the ion beam parallel to the sample surface and suitable for EBSD data collection (Fig. 23). Depending on the design of the system, this might involve moving the sample automatically between two working geometries.

By repeating the process of acquiring an EBSD dataset and exposing a new surface, it is possible to generate a 3D representation of the microstructure within the analysed volume. To get a good resolution of the data, it is often required to have data from several tens of slices (potentially more than a hundred) which can make it a time-consuming process.

An example from a dataset collected with a step size of 0.2 μm in the x, y and z directions is shown in Fig. 24. As shown, this technique can be useful to study boundaries and grain shapes.

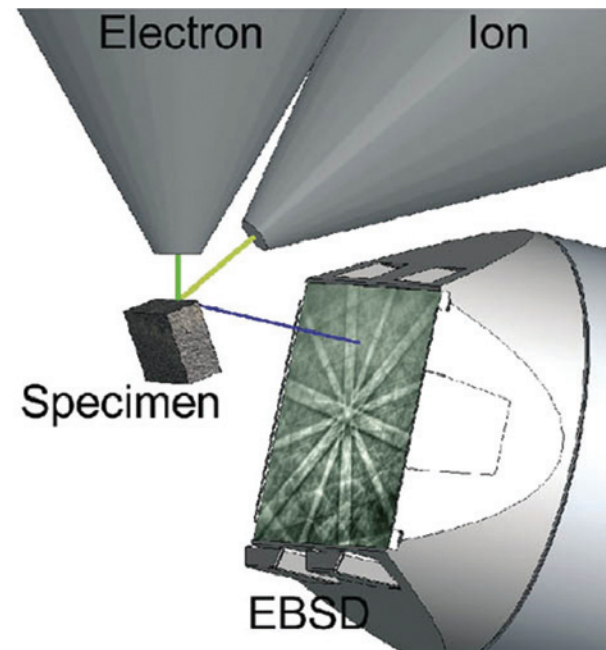

Fig. 23. Schematic showing an example of the EBSD geometry for a FIB-SEM used for 3D-EBSD analysis.

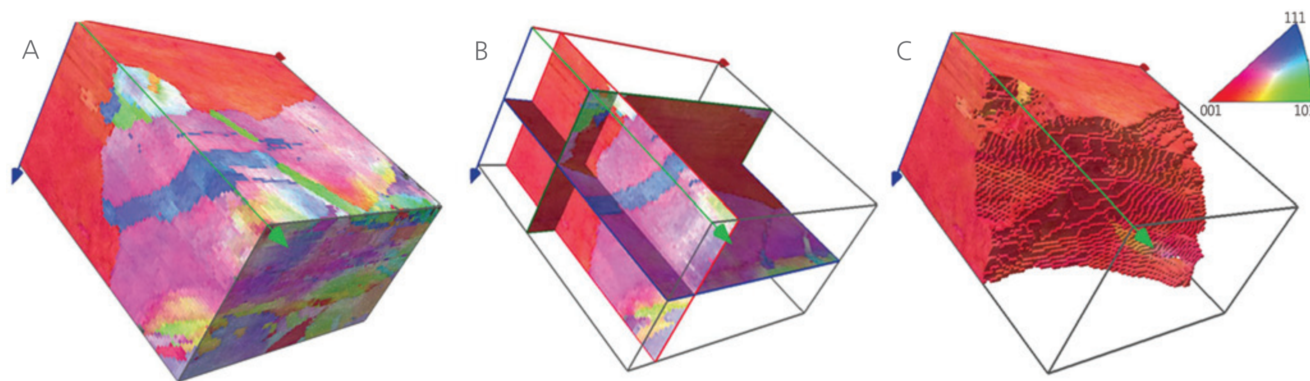

Fig. 24. Example shows 3D EBSD analysis through a Cu sample;

A) Reconstructed and processed 3D orientation map;

B) Cross-sections in X, Y and Z planes;

C) A single grain selected and highlighted.

Transmission Kikuchi Diffraction (TKD)

Conventional EBSD is done on a tilted sample (Fig. 1), which typically means that the spatial resolution is limited by the longer working distance (WD). This longer WD is required in order to physically get the tilted sample placed in a suitable geometry with respect to the SEM pole piece and the EBSD detector. Secondly and potentially more important, due to the high sample tilt, the resolution in the direction perpendicular to the tilt axis (downhill) is reduced by nearly a factor of 3 due to the enlarged interaction volume.

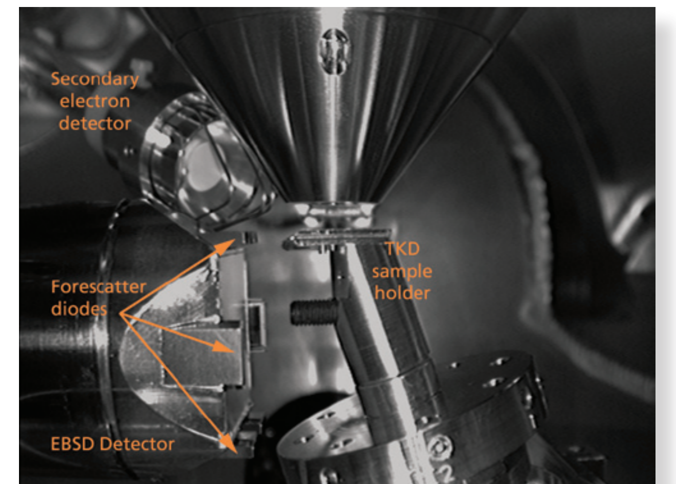

Fig. 25. The geometry of a system set up for TKD. Thinned samples are mounted horizontally in the SEM chamber and positioned towards the top of the EBSD detector's phosphor screen.

To improve the spatial resolution within the EBSD data, it is advisable to use lower probe currents, lower kV, and to try to work at a shorter WD to improve the spatial resolution of the SEM. There are however practical limits to how the sample can physically be positioned. Reducing the kV or current requires a more sensitive EBSD detector, otherwise the data acquisition time increases significantly, which leads to drift and stability problems.

Recently an alternative technique to improve the spatial resolution has been demonstrated, and is becoming popular. The technique is called Transmission Kikuchi Diffraction (TKD or t-EBSD), and it makes use of a conventional EBSD system, however with the sample placed in a different geometry (Fig. 25).

For TKD, the sample must be thinned so that it is electron transparent (as for TEM). In this case, the scattering event takes place on the lower surface of the sample as the electron beam exits from the sample. This means that the sample can be placed at a shorter WD than for conventional EBSD, which in itself gives an improvement in the spatial resolution. Secondly, due to the geometry, it is generally not required to tilt the sample more than 10 degrees (dependent on the setup) to be able to collect a good collection geometry while keeping the EBSD detector in its normal geometry. Again, this leads to an improvement in spatial resolution.

TKD is still a new technique but it has already proven very useful for acquiring orientation data from materials with a small grain size or high level of deformation, as shown by the maps on the front cover and the back page (Fig. 26).

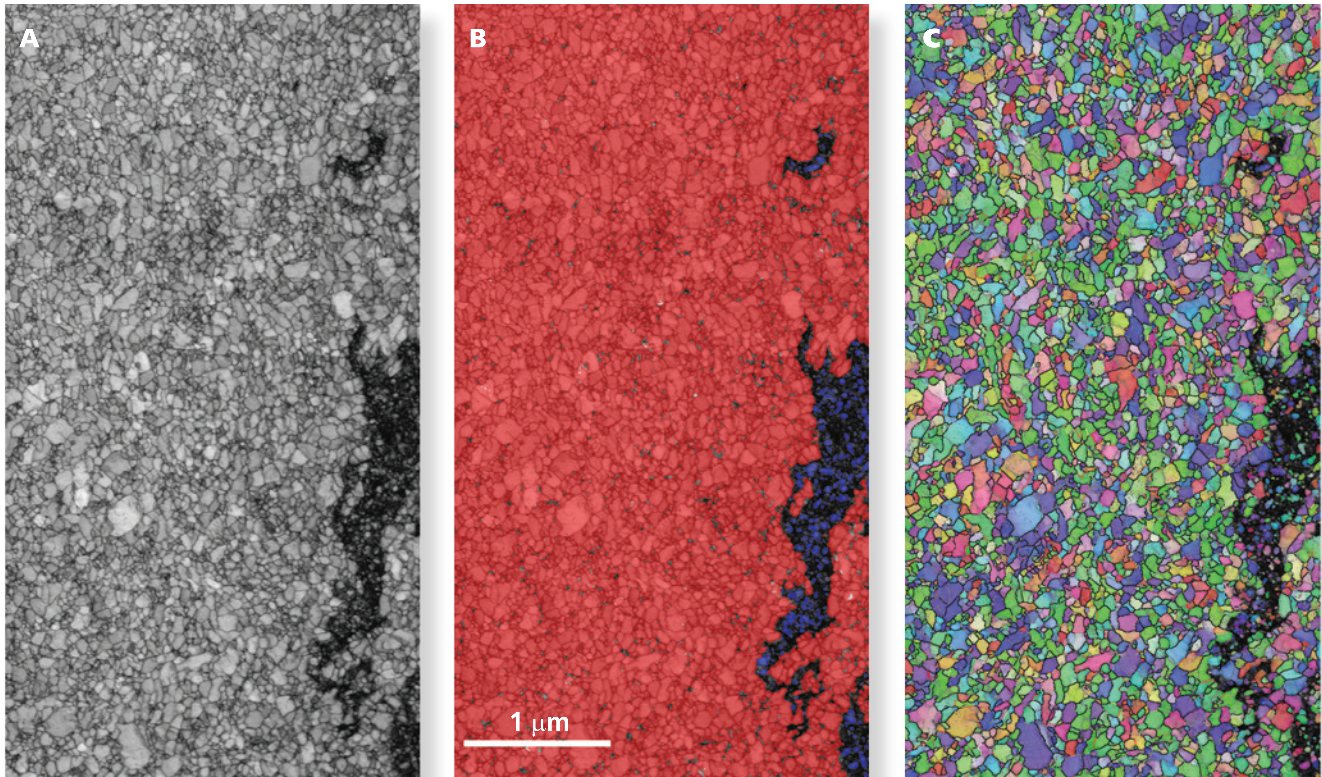

Fig. 26. TKD characterisation of a deformed duplex stainless steel sample.

A) The pattern quality map showing the fine grain size and the significantly poorer quality patterns in certain areas.

B) The phase map which shows ferrite (BCC) in red and austenite (FCC) in blue, and highlights that the poorer quality patterns are associated with the areas occupied by the FCC phase, in which the TKD technique can resolve only the larger grains.

C) The orientation map that shows the lack of texture in this sample, but also shows the deformation within the larger grains (> 100 nm) exhibited by substantial intra-grain orientation variations.

Data courtesy: Pat Trimby, Yang Cao and Saritha Samudrala, University of Sydney.

www.oxford-instruments.com/EBSD

The materials presented here are summary in nature, subject to change, and intended for general information only. Additional details are available. Oxford Instruments NanoAnalysis is certified to ISO9001, ISO14001 and OHSAS 18001. AZtec and Tru-I are Registered Trademarks of Oxford Instruments plc, all other trademarks acknowledged. © Oxford Instruments plc, 2015. All rights reserved. Document reference: OINA/EBSD Explained/0215.

The Business of Science®